Man-portable, real-time, passive millimeter-wave imaging sensor

Charles E. Harrity*[a], Dominic Marinucci [a], Samhit Dontamsetti [a], Timothy Creazzo [a], Sabrina Rosenthal [a], Dylan Laplace [a], Robert Wilcox [a], Eric Shaw [a], Kevin Shreve [a], Zachary El-Azom [a], Chad Newkirk [a], Melvin Tejada [a], Jesse Semmel [a], Christopher Schuetz[a], Shouyuan Shi [ab] and Dennis W. Prather [ab]

[a] Phase Sensitive Innovations, Inc., 116 Sandy Drive, Newark, DE, USA;

[b] University of Delaware, Newark, DE, USA 19716

ABSTRACT

Passive millimeter-wave (mmW) imaging has applications ranging from degraded visual environment mitigation and stand-off security screening to next generation high speed communication systems. Traditional radiometric imaging approaches at these frequencies require a large aperture and a correspondingly large lens or, in the case of a phased array approach, large and bulky RF components to support the required analog RF processing. One technique for realizing low size weight and power (SWaP) radio frequency (RF) systems is the employment of optical techniques, which can allow for the replacement of RF components and cables with lightweight optical components and fibers. In particular, optical up-conversion techniques are well suited for the development of a low-SWaP radiometric imager. The RF photonic imager we have developed consists of a distributed phased array of up-conversion modules in which each element leverages an electro-optic modulator to perform optical up-conversion. This technique upconverts the RF signal to the optical domain to enable optical processing of the RF signal. Optical processing of the RF signal allows for RF beamforming with a near unlimited beam-bandwidth product with minimal power consumption. In this work, each system has been addressed to reduce the size and weight of the sensor, resulting in a man-portable imaging sensor which operates at video rates. Operating at 85 GHz and weighing under 25 lbs, this sensor represents a significant improvement in SWaP compared to previously reported imaging sensors.

Keywords: mmW, millimeter-wave, RF Photonics, optical up-conversion, passive mmW imaging, radiometric imaging

1. INTRODUCTION

Imaging technologies are critical in applications ranging from security screening to automation. Modalities such as visible and infrared benefit from illumination from the sun or strong thermal emissions. RF imaging systems, specifically those in the millimeter wave regime, have been limited due to weak natural emissions, poor resolution and hardware availability[1]. Interest in this spectrum is based on a unique capability of passing through common obscurants including dust and fog as well as materials such as plastics and clothing[2]. To offset the limitations of natural illumination sources, many mmW sensors use active illumination. However, these tend to be limited in implementation, require the subject to adopt specific positions[3], require close proximity to the sensor and have slow scanning speeds[4]. A passive sensor overcomes these limitations but requires a significant increase in sensitivity to surpass the power limitations. Traditional detection systems use lenses to focus beams to a sensor and as a result will scale volumetrically in size[5]. Phased array systems can be used but require phase synchronization between elements and require significant signal processing to extract useful information. An alternate approach is to use a technique known as optical-up conversion where the RF signal is modulated onto a laser[6]. This has the advantage of using optical lenses to perform real-time processing of the RF signal with no power consumption. When paired with a phased array, the size and weight of the imaging sensor can also be drastically reduced.

In this paper a passive mmW imaging sensor is presented which utilizes a densely packed phased array and optical conversion to achieve a low size, weight and power (SWaP) while also having the sensitivity necessary for imaging passively indoors. A phase control system which tracks and updates the phases of each channel using a spatial phase control loop (SPCL)[7] is utilized to synchronize each array element. A commercially available short-wave infrared (SWIR) camera receives the processed image output by the optical processor.

*harrity@phasesensitiveinc.com; phone 1 302 286-5191; phasesensitiveinc.com

Terahertz, RF, Millimeter, and Submillimeter-Wave Technology and Applications XVIII,
edited by Laurence P. Sadwick, Tianxin Yang, Proc. of SPIE Vol. 13365,
133650P · © 2025 SPIE · 0277-786X · doi: 10.1117/12.3042219

2. METHOD

System Design

The optical up-conversion technique uses a high-speed electro-optic modulator to encode the phase and amplitude information of the RF signal onto an optical signal in the form of sidebands. Once converted to optics the signal is sent over optical fiber to an optical processer which performs a Fourier transform of the up-converted signal focusing the signal to spots which are received by a SWIR camera. Shown in Fig. 1, the RF waves marked in red, and blue can be traced from left to right to form focused spots in the optical domain.

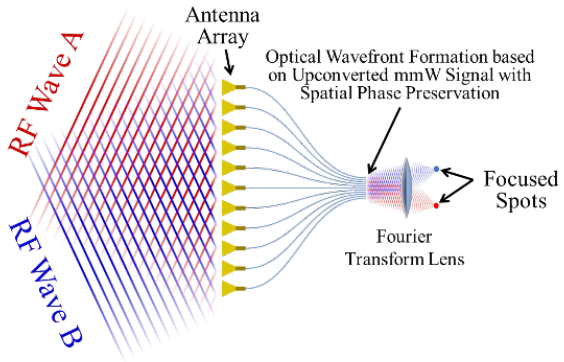

Fig. 1. Diagram illustrating optical beamforming of the RF signal

Following the RF path, the signal enters the antenna and is amplified by a pair of low noise amplifiers (LNAs), critically these offer a low noise figure, less than 6 dB, and high gain which is nominally 63 dB. The RF signal is transitioned to a fiber coupled high-speed LiNbO3 modulator[8], which mixes the RF signal with the optical carrier, generating sidebands. The output of each modulator is directed to a 2-dimensional fiber array, the positions of which are scaled according to the antenna positions of the RF front end. A micro-lens array, whose pitch matches the fiber array, is used to collimate the beams of each fiber. The output is then sent into a circulator, the output of which is coupled with a narrow band-pass filter. The filter strips off a single sideband sending it to a series of Fourier transform lenses and is imaged by the SWIR camera while rejecting the carrier and the opposite sideband. The rejected light is sent back through the circulator to a photodiode array, with a detector corresponding to each fiber. A reference beam is overlaid on the entire PD, mixing with the carrier signal from each fiber. A sawtooth function is applied to the reference using a phase modulator. The mixing of the optical signals generates a sine wave whose phase offset is proportional to the phase drift of the individual channel[9]. The Analog-to-Digital Phase Error Correction board (APEC) measures the phases, calculates the offset and sends this to back to each up-conversion channel, creating the SPCL and correcting the phases in real-time. The interactions of these systems can be seen in Fig. 2. The dotted orange lines show the RF signal path and the solid blue lines show the optical signal path. Not described in the discussion above is the optical feed network, which consists of a laser, erbium doped fiber amplifier (EDFA), filter, and optical splitters to distribute the optical signal to the up-conversion channels.

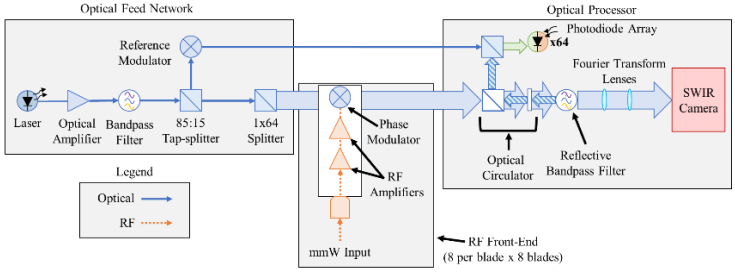

Fig. 2. System block diagram

Calibration, Beam-steering and Image Processing

The SPCL monitors and updates the phases of each element in real time, however each element will have an inherent phase offset relative to each other channel. Therefore, the system must be calibrated to ensure that the energy form each channel interferes coherently to form an image. The calibration simply corrects for this phase offset by applying a phase profile

across the entire array. Similarly, a phase profile can be applied to enable non-mechanical beam-steering of the array, shifting the image vertically or horizontally or adjusting the focal distance of the array[10].

The data collected with this system uses several image processing techniques to enhance the imagery and reduce the noise. An optical technique, similar to Dicke switching is used, where the system alternates between "phased locked" and "phase scrambled" frames. The frame pairs are subtracted to remove the background noise[11]. A pre-normalization is performed frame to frame to reduce flicker and compensate for shifts in power or wavelength of the seed laser and EDFA. A weighted temporal pre-average is applied, typically averaging 10 frames, to further reduce the noise. Finally, a background image is taken and subtracted from the final image. The background can use either an RF absorber to isolate the background generated by the imager or can be an image taken of the scene to isolate new and moving objects.

3. SYSTEM PERFORMANCE AND RESULTS

Improvements in the Fiber Bundle and Microlens Alignment

The accuracy of the fiber placement in the 2D fiber bundle and its alignment to the microlens array are critical to the performance of the system. The microlens array positions are lithographically defined, making their positions accurate to +/- 1 um. The fiber array typically will have much larger inaccuracies. The 2D fiber arrays used in this system are made using a faceplate which is fabricated through photolithography. While this accurately defines the initial starting position, over etching and placement error result in fibers which are misaligned with the lithographically defined positions. The alignment of the fiber center relative to the microlens array center will change the direction of the beam for that channel in the optical processor, which results in a shift of the corresponding focused spot in the image plane of the optical processor. A figure of merit for evaluating the alignment quality of the fibers in the fiber array is the percentage of image area in which all of the beams overlay. For perfect alignment of all fiber array elements, the image area FOM is 100%. In previous systems, we found that that the image area overlay was only 4.4% limited by the alignment errors mentioned above. In this new system, a new fiber array with better alignment tolerance demonstrated an image area FOM of 73.3%.

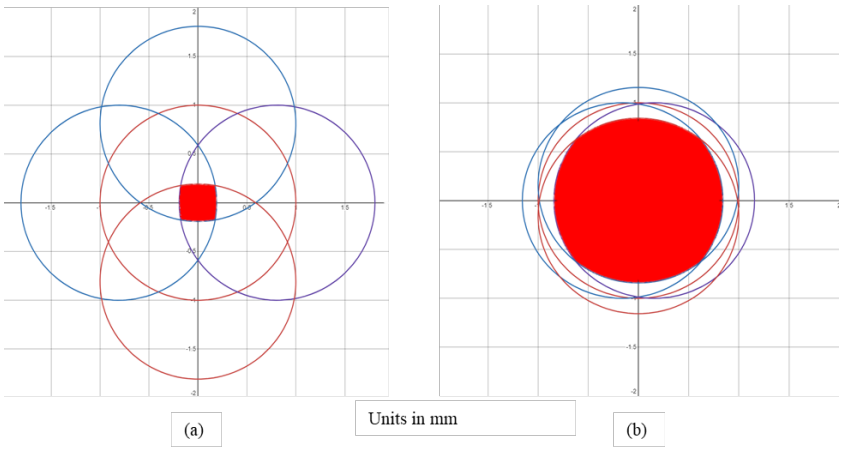

Fig. 3. Visualization of overlay in previous arrays (a), new array (b).

The practical implication of the fiber bundle improvement is the efficiency in which the optical power is used to generate the final output image. With the beam overlay improvement, the amount of optical power incident on the camera increased significantly, which offered an opportunity to further optimize the system. While it is possible to compensate for increased optical power by reducing the integration time of the camera, this also reduces the ability to mitigate noise in the image due to limitations of the camera's speed and saturation point. An alternative option is to decrease the amount of optical power in the system by removing the EDFA, which is a source of optical noise, power consumption, additional weight, and heat within the system. Removing the EDFA enables a reduction in the overall power consumption of the system by 16 W.

Specifications

A 64-channel phased array video-rate imaging system was constructed using the optical up-conversion approach. The system can be specified in terms of imaging (RF) performance and sensitivity. The field of view and angular resolution of the system are defined by the mechanical design of the system. The angular resolution is proportional to the aperture size and was calculated to be 2.2 degrees. The field of view is dependent on the RF antenna design in the up-conversion blade and was measured to be 17-degrees. The center frequency of operation is 85 GHz and the 3-dB bandwidth is 6 GHz, both are determined by the specification and packaging of the LNAs within the up-conversion blade. The framerate after processing is 20 Hz, and the noise equivalent temperature difference (NETD) is less than 1K. The system measures 10" x 10" x 12.5", without including an optional visible camera mounted and handles, weighs 24.8 lbs and has a power draw of 60.2 W. The system is shown in Fig. 4 (g) with sample imagery Fig 4 (a), (c), (e) along with corresponding visible images Fig. 4 (b), (d), (f). Featured images show passive mmW image of a hand, and ice pack and a hand covering an icepack all recorded at a range of 0.3 meters. In images (a) and (e), the individual fingers can be resolved.

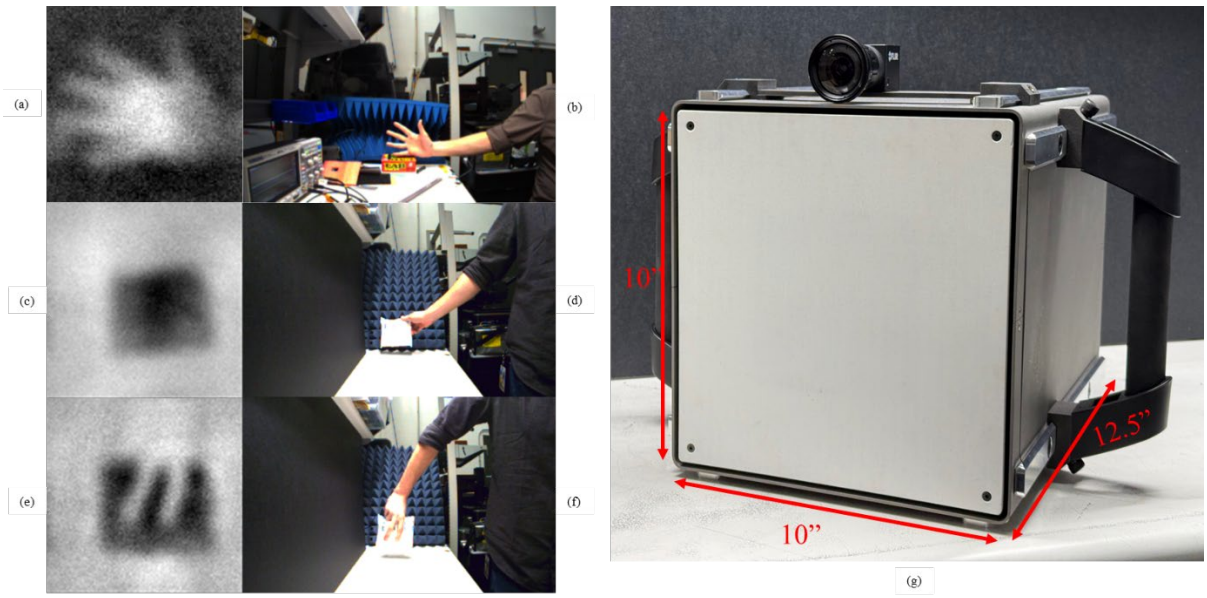

Fig. 4. (a) mmW image of hand; (b) corresponding visible image; (c) mmW image of an ice pack; (d) corresponding visible image; (e) mmW image of fingers spread across ice pack; (g) passive mmW imager

4. CONCLUSION

In this paper we presented a low SWaP, man portable passive mmW imager that uses optical up-conversion to image in real-time. Improvements to the sub-systems, particularly the 2D fiber array, yielded a reduction in power consumption without sacrificing performance. The system operates at 85 GHz, has an NETD below 1 K, a 20 Hz frame rate and a 17-degree field of regard. The system has applications ranging from degraded visual environment mitigation to standoff security screening and can be fused with other imaging modalities to enhance current capabilities.

ACKNOWLEDGEMENTS

This work was partially funded by the Office of Naval Research in addition to other U.S. government contracts whose research was leveraged for this work. The authors would also like to acknowledge to entire team at Phase Sensitive Innovations as well as our collaborators at the University of Delaware.

REFERENCES

[1] Yujiri, L., Shoucri, M. and Moffa, P., "Passive millimeter-wave imaging," IEEE Microw. Mag. 4(3), 39–50 (2003); http://dx.doi.org/10.1109/MMW.2003.1237476.

[2] Zelong Xiao, Jianzhong Xu, and Taiyang Hu., "Research on the transmissivity of some clothing materials at millimeter-wave band," 2008 Int. Conf. Microw. Millim. Wave Technol., 1750–1753, IEEE, Nanjing, China (2008); http://dx.doi.org/10.1109/ICMMT.2008.4540812

[3] Wang, Z., Chang, T. and Cui, H.-L., "Review of Active Millimeter Wave Imaging Techniques for Personnel Security Screening," IEEE Access 7, 148336–148350 (2019); http://dx.doi.org/10.1109/ACCESS.2019.2946736.

[4] Cooper, K. B., Dengler, R. J., Llombart, N., Bryllert, T., Chattopadhyay, G., Schlecht, E., Gill, J., Lee, C., Skalare, A., Mehdi, I. and Siegel, P. H., "Penetrating 3-D Imaging at 4- and 25-m Range Using a Submillimeter-Wave Radar," IEEE Trans. Microw. Theory Tech. 56(12), 2771–2778 (2008); http://dx.doi.org/10.1109/TMTT.2008.2007081.

[5] Williams, T. D. and Vaidya, N. M., "A compact, low-cost, passive MMW security scanner," presented at Defense and Security, (2005); http://dx.doi.org/10.1117/12.603662.

[6] Wilson, J. P., Schuetz, C. A., Dillon, T. E., Yao, P., Harrity, C. E. and Prather, D. W., "Passive 77 GHz millimeter-wave sensor based on optical upconversion," Appl. Opt. 51, 4157 (2012); http://dx.doi.org/10.1364/AO.51.004157

[7] Prather, D. W., Murakowski, J. A., Schuetz, C., Shi, S., Schneider, G. J., Harrity, C., Aranda, Z. D., Marinucci, D., Hallak, A., Zablocki, M., Gallion, M., Dontamsetti, S., Goodman, B. J., Semmel, J. and Lawrence, R., "Millimeter-Wave and Sub-THz Phased-Array Imaging Systems Based on Electro-Optic Up-Conversion and Optical Beamforming," IEEE J. Sel. Top. Quantum Electron. 29(5: Terahertz Photonics), 1–14 (2023); http://dx.doi.org/10.1109/JSTQE.2023.3306953.

[8] Macario, J., Yao, P., Shi, S., Zablocki, A., Harrity, C., Martin, R. D., Schuetz, C. A. and Prather, D. W., "Full spectrum millimeter-wave modulation," Opt. Express 20(21), 23623 (2012); http://dx.doi.org/10.1364/OE.20.023623.

[9] Martin, R. D., Schuetz, C. A., Prather, D. W. and Dillon, T. E., "Controlling the phase of optical carriers," US8159737B2.

[10] Dillon, T. E., Schuetz, C. A., Martin, R. D., Mackrides, D. G., Curt, P. F., Bonnett, J. and Prather, D. W., "Nonmechanical beam steering using optical phased arrays," presented at SPIE Security + Defense, (2011); http://dx.doi.org/10.1117/12.898356.

[11] Martin, R. D., Schuetz, C., Prather, D. W. and Dillon, T. E., "Coherence Switching," US20120288214A1 (2016).